Oxygen Diffusion in Bilayer Polymer Films

Lars Poulsen,[†] Ingo Zebger,[†] Pentti Tofte,[‡] Markus Klinger,[†] Ole Hassager,[‡] and Peter R. Ogilby*,[†]

Department of Chemistry, University of Aarhus, Langelandsgade 140, DK-8000 Århus, Denmark, and Department of Chemical Engineering, Technical University of Denmark, DK-2800, Lyngby, Denmark

Received: August 4, 2003; In Final Form: October 17, 2003

Experiments to quantify oxygen diffusion have been performed on polymer samples in which a film of poly(ethylene-*co*-norbornene) was cast onto a film of polystyrene which, in turn, was cast onto an oxygen-impermeable substrate. In the technique employed, the time evolution of oxygen transport through the film of poly(ethylene-*co*-norbornene) and into the polystyrene film was monitored using the phosphorescence of singlet oxygen as a spectroscopic probe. To analyze the data, it was necessary to solve Fick's second law of diffusion for both polymer films. Tractable analytical and numerical solutions were obtained for the problem. Moreover, the numerical solution is sufficiently general that it can be used to simulate oxygen concentration profiles in films consisting of more than two layers. Data obtained from the bilayer films yield a diffusion coefficient for oxygen in poly(ethylene-*co*-norbornene) that is consistent with diffusion coefficients independently obtained from monolayer films and bulk samples.

Introduction

The ability to quantify the diffusion of small molecules through polymer films has widespread ramifications that influence problems of both fundamental as well as applied interest.[1−4] The diffusion of molecular oxygen is particularly important given that oxygen is ubiquitous in the earth's atmosphere and in materials exposed to the earth's atmosphere. Moreover, oxygen has many unique properties that distinguish it from other small molecules.[5] Of particular importance, certainly with respect to polymers and polymeric barrier materials, is the key role played by oxygen in the degradation of polymers and of items that a given polymer is intended to protect (e.g., food encased in a polymeric package).[6,7]

Approximately 10 years ago, we developed a spectroscopic tool to quantify the diffusion coefficient of oxygen in polymer films.[8] We have since used this tool to address a variety of issues related to the diffusion of oxygen in glassy polymers.[9−11] In our approach, oxygen sorption into the polymer is monitored using the near-infrared phosphorescence of singlet molecular oxygen, $O_2(a^1\Delta_g)$, as the probe ($O_2(a^1\Delta_g) \rightarrow O_2(X^3\Sigma_g^-) + h\nu(\sim 1270$ nm)). In these studies, singlet oxygen has been produced by energy transfer to ground-state oxygen, $O_2(X^3\Sigma_g^-)$, from a photosensitizer dissolved in the polymer. Thus, upon exposure of a degassed polymer sample to an ambient atmosphere of oxygen, the time-dependent phosphorescence signal observed reflects the rate of oxygen sorption by the sample. For a sample of known thickness, l, the data yield the oxygen diffusion coefficient, D, when examined using a solution to Fick's second law of diffusion.[8−11]

In developing this technique, one of our first control experiments was to establish that, at the concentrations used, the presence of the singlet oxygen sensitizer does not influence the diffusion coefficients recorded. Although we indeed determined that the sensitizer does not alter properties of the polymer that influence the propagation of oxygen through the material,[8] there are nevertheless many polymeric materials and/or conditions in which it is difficult or undesirable to use a dissolved sensitizer. Under these latter conditions, singlet oxygen could similarly be produced in a photosensitized reaction upon irradiation of a chromophore inherent to the macromolecule itself. This approach could be viable in a material such as polycarbonate, for example, from which a singlet oxygen phosphorescence signal has been observed upon irradiation of the polymer.[12] Alternatively, singlet oxygen could also be produced in some sensitizer-free polymers upon irradiation into the oxygen−polymer charge-transfer absorption band.[13,14] In both of these cases, the intensity of the singlet oxygen phosphorescence signal observed would be proportional to the concentration of ground-state oxygen in the polymer film and, as such, could be used to monitor oxygen sorption into the sample.

Another approach by which this spectroscopic technique could be used to quantify oxygen diffusion in sensitizer-free samples involves the use of a second, well-characterized film that contains a singlet oxygen sensitizer. This second *sensor* film would simply be used to monitor oxygen diffusion through a sensitizer-free *sample* film. In short, for a system in which the sample film has been cast onto the sensor film, the rate of oxygen sorption into the sensor film would depend on the oxygen diffusion coefficient in the sample film (Figure 1). This general approach is not new and, to our knowledge, was first applied to the problem of oxygen diffusion by Petrak.[15] In this original study, the rate of oxygen sorption into the sensor film was monitored using a chemical reaction to trap singlet oxygen. In a recent variation of this technique, Winnik and colleagues monitored oxygen-dependent changes in the luminescence intensity of a dye embedded in the sensor layer.[16]

There are several potentially complicating aspects of this approach involving a separate sensor film. It must first be possible to place the sample film on top of the sensor film and yet maintain both a homogeneous interface between the films and a constant film thickness over the entire area exposed to oxygen. Second, the appropriate equations for diffusion that must be solved and applied are nontrivial. On the other hand, multilayer polymer films play an increasingly important role

* To whom correspondence should be addressed. E-mail: progilby@chem.au.dk.
[†] University of Aarhus.
[‡] Technical University of Denmark.

10.1021/jp0362739 CCC: $25.00
Published on Web 11/20/2003

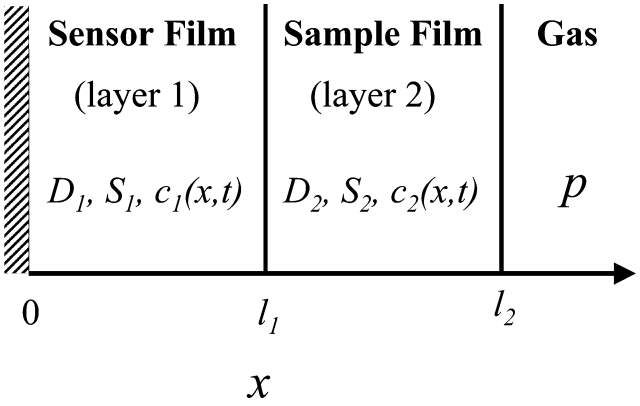

Figure 1. Geometry of the bilayer experiment. A well-characterized sensor film, layer 1, which contains a singlet oxygen sensitizer, is deposited onto an oxygen-impermeable substrate (e.g., a glass plate). The sample film of thickness $l_2 - l_1$, layer 2, is deposited on top of the sensor film of thickness l_1. Upon exposure of the degassed bilayer to a specific pressure of oxygen, p, the rate of oxygen sorption into the sensor layer is determined by the rate of oxygen transport through the sample layer. Each layer is characterized by a diffusion coefficient for oxygen, D, and oxygen solubility, S, and a time-dependent oxygen concentration profile, $c(x,t)$.

in modern technology with widespread applications, particularly in the packaging industry.[17,18] Thus, efforts to address these problems are readily justified.

Of course, problems associated with the direct deposition of the sample film onto the sensor film could be avoided if the diffusion experiment is performed under conditions in which there is a space between the sample and sensor films. Thus, oxygen would diffuse through a free-standing sample film to reach the sensor film. The geometry of this latter experiment is similar to that used in the traditional permeation (i.e., time lag) experiments.[2,16] Although this free-standing geometry indeed has desirable aspects, it also has limitations. For example, to avoid pressure-induced distortions that would perturb and potentially break the sample film, it is necessary to have a second gas in the system (e.g., nitrogen) to moderate pressure differences across the sample film. In this regard, we have independently shown that oxygen diffusion coefficients can be significantly perturbed when a second molecule, such as nitrogen, is cosorbed into the polymer.[10,11]

For the present study, we therefore set out to apply our singlet oxygen spectroscopic probe to the problem of quantifying oxygen diffusion in contiguous bilayer films.

Experimental Section

The instrumentation and approach used to spectroscopically monitor the time evolution of oxygen sorption into polymer films have been described previously.[8−11]

Poly(ethylene-*co*-norbornene) was obtained as a gift from Hoechst Ticona, Germany. The material was obtained in the form of pellets and was used without further purification. In the nomenclature system of Hoechst Ticona, this cyclo-olefin copolymer is known as TOPAS 8007. In an independent study, we ascertained that it consists of 35 mol % norbornene and 65 mol % ethylene, has a weight average molecular weight of 116 000 g/mol, and has a glass transition temperature of 79 °C.[19] Polystyrene (Aldrich), with a weight average molecular weight of 280 000 g/mol, was obtained in the form of pellets and used without further purification.

The singlet oxygen sensitizer used in the polystyrene sensor film was *meso*-tetraphenylporphine, TPP (Aldrich, used as received). The amount of sensitizer used was adjusted to yield an absorbance at 420 nm of ∼0.4−0.6 in the final polymer film. This corresponds to a sensitizer concentration of $\sim 1-2 \times 10^{-3}$ M in the film. At such concentrations, the presence of the sensitizer does not perturb oxygen diffusion in polystyrene.[8]

Preparation of the Bilayer Films. The sensor layer was prepared by first dissolving TPP and the polystyrene pellets in benzene. The amount of polymer generally used was 10−20 wt %. The benzene solutions of the polymer and sensitizer were maintained at 25 °C for 24 h to achieve homogeneity and then were spin cast onto glass plates. A Headway Research model EC101DT-R790 photoresist spinner, operating between 3000 and 7000 rpm, was used to cast the films. After the films stood for 24 h under ambient atmosphere, they were placed under vacuum for 24 h to facilitate the removal of the remaining solvent. Finally, the films were annealed at 50 °C for 1 h under vacuum using a Lab-Line Duo-Vac oven (model 3620-ST-1).

The film thickness was quantified using interference fringes that appear in the IR spectrum of the sample. Specifically, using a microscope attached to a Fourier transform IR spectrometer, the reflection−absorption spectrum of the polymer film was recorded (i.e., the sample was placed on a reflective gold mirror). A Bruker IRscopeII connected to a Bruker IFS-66v/S spectrometer was used. In a given spectrum, the interference fringes were evaluated over the range ∼1500−2300 cm^{-1}. The film thickness, l, was obtained from the period of the interference fringes, $\Delta\nu$, via the relation $l = (2n\Delta\nu)^{-1}$, where n is the refractive index of the polymer.[20,21]

To prepare the sample layer, the pellets of poly(ethylene-*co*-norbornene) were first dissolved in cyclohexane. Again, the amount of polymer used was generally 10−20 wt %. This solution was then spin cast onto the polystyrene film using the photoresist spinner. The films were held at ambient temperature and pressure for 24 h and then placed in a vacuum for an additional 24 h. Finally, the bilayer films were annealed at 50 °C for 24 h under vacuum. The resultant films were clear and homogeneous.

The thickness of the bilayer film was likewise quantified with the interference fringe method. In this case, an average of the polystyrene and poly(ethylene-*co*-norbornene) refractive indices was used. The thickness of the poly(ethylene-*co*-norbornene) sample layer was determined from the difference between the thickness of the bilayer film and the thickness of the polystyrene sensor layer. The bilayer films produced generally consisted of a polystyrene sensor layer that was ∼10 μm thick and a poly(ethylene-*co*-norbornene) sample layer that was ∼5 μm thick.

Results and Discussion

1. Solutions to Fick's Second Law of Diffusion. If one is to investigate, in a bilayer system, how the sorption of oxygen into one layer can be modulated by the diffusion through a second layer, it is necessary to solve Fick's second law of diffusion for both layers in the system (eqs 1 and 2)[22]

$$\frac{\partial c_1}{\partial t} = D_1 \frac{\partial^2 c_1}{\partial x^2} \qquad \text{for} \quad 0 \le x \le l_1 \tag{1}$$

$$\frac{\partial c_2}{\partial t} = D_2 \frac{\partial^2 c_2}{\partial x^2} \qquad \text{for} \quad l_1 \le x \le l_2 \tag{2}$$

As illustrated in Figure 1, the first layer (the sensor) has a thickness of l_1, whereas the second layer (the sample) has a thickness of $l_2 - l_1$.

The boundary conditions for this problem are given in eqs 3−7

$$c_2(l_2,t) = S_2 p \qquad \text{at} \quad t > 0 \tag{3}$$

$$\frac{c_1(l_1,t)}{S_1} = \frac{c_2(l_1,t)}{S_2} \qquad \text{at} \quad t > 0 \tag{4}$$

$$D_1 \frac{\partial c_1}{\partial x}(l_1,t) = D_2 \frac{\partial c_2}{\partial x}(l_1,t) \qquad \text{at} \quad t > 0 \tag{5}$$

$$\frac{\partial c_1}{\partial x}(0,t) = 0 \qquad \text{at} \quad t > 0 \tag{6}$$

$$c_1(x,0) = c_2(x,0) = 0 \qquad \text{all} \quad x \tag{7}$$

Equation 3 states that the oxygen concentration, c_2, at the surface of the outer layer, l_2, is always proportional to the external pressure of oxygen, p (i.e., it is assumed that Henry's law is obeyed). In this case, the proportionality constant is the solubility of oxygen, S_2, in the sample layer. Equation 4 states that the partial pressure of oxygen does not change (i.e., is continuous) across the interface between layers 1 and 2. In short, we assume equilibrium at the interface. In eq 5, it is stipulated that the oxygen flux is likewise continuous across the interfacial boundary at l_1. It is assumed there is no diffusion through the glass plate at $x = 0$ (eq 6) and, finally, both layers are assumed to be free of oxygen at $t = 0$ (eq 7).

Analytical Solution. The equivalent boundary value problem in heat conduction has been solved using Laplace transformations.[23] In turn, this approach has been applied to the problem of gas transport in multilayer films.[22,24] For our present work, we use an alternative approach in which an expansion in eigenfunctions is used to represent the solution.[25]

To more readily accommodate an analytical solution to this diffusion problem, we first render the model dimensionless by establishing dimensionless variables and constants. The resultant partial differential equations can then be transformed and solved as a Sturm−Liouville problem.[25] To this end, dimensionless oxygen concentrations in the respective layers, y_i, are defined as shown in eqs 8 and 9

$$y_1 = 1 - \frac{c_1}{S_1 p} \tag{8}$$

$$y_2 = 1 - \frac{c_2}{S_2 p} \tag{9}$$

Note that, at $t = 0$, the concentrations y_i have a value of 1. However, when equilibrium with the ambient atmosphere is reached and the concentrations of sorbed gas are at a maximum, y_i is 0. We also define dimensionless parameters that refer to both the position in the polymer film ($z = x/l_2$ and $\alpha = l_1/l_2$) as well as time ($\tau = tD_2/l_2^2$).

With these variables, the expressions for Fick's second law of diffusion, eqs 1 and 2, become

$$q^2 \frac{\partial y_1}{\partial \tau} = \frac{\partial^2 y_1}{\partial z^2} \qquad \text{for} \quad 0 \le z \le \alpha \tag{10}$$

$$\frac{\partial y_2}{\partial \tau} = \frac{\partial^2 y_2}{\partial z^2} \qquad \text{for} \quad \alpha \le z \le 1 \tag{11}$$

where $q = (D_2/D_1)^{1/2}$. These differential equations can now be transformed into a Sturm−Liouville problem by expressing the dependent variables y_1 and y_2 as products of functions that depend on position and time (eqs 12 and 13)

$$y_1 = \sum_{n=1}^{\infty} f_{1,n}(z) g_{1,n}(\tau) \tag{12}$$

$$y_2 = \sum_{n=1}^{\infty} f_{2,n}(z) g_{2,n}(\tau) \tag{13}$$

In this Sturm−Liouville problem with the specified boundary conditions, the eigenvalues, λ_n, are determined as the real solutions to the following expression

$$qS \cot((1-\alpha)\lambda_n^{1/2}) = \tan(q\alpha\lambda_n^{1/2}) \tag{14}$$

where S is the ratio of the oxygen solubilities in the respective layers ($S = S_2/S_1$). This was accomplished using a Newton iteration[26] implemented in a MATLAB routine.[27] In turn, the position-dependent eigenfunctions, $f_{i,n}(z)$, can be expressed as

$$f_{i,n}(z) = \begin{cases} \sin((1-\alpha)\lambda_n^{1/2}) \cos(qz\lambda_n^{1/2}) & 0 \le z \le \alpha \quad (i=1) \\ \sin((1-z)\lambda_n^{1/2}) \cos(q\alpha\lambda_n^{1/2}) & \alpha \le z \le 1 \quad (i=2) \end{cases} \tag{15}$$

which yield concentration profiles for oxygen in the polymers at a specified time, t, after exposure to the gas at a given pressure, p. The solutions to the partner equations to the Sturm−Liouville problem is straightforward and yields

$$g_{i,n}(\tau) = a_{i,n} \exp(-\lambda_n \tau) \qquad 0 \le \tau \le \infty \tag{16}$$

where $i = 1, 2$ and $n = 1, 2, \ldots, \infty$.

To model our experimental data, however, what is explicitly needed is an expression for the time-dependent sorption of oxygen in the sensor layer. This corresponds to the integral in eq 17, where $M(t)$ is the amount of oxygen sorbed at time t

$$M(t) = \int_{x=0}^{x=l_1} c_1(x,t)\, dx \tag{17}$$

With respect to the dimensionless formulation, the analogous expression is obtained by integrating eq 12 over the limits that likewise correspond to the thickness of the sensor layer. Once again, relying on eq 14, this yields

$$\int_0^{\alpha} f_{1,n}(z)\, dz = \frac{S}{\lambda_n^{1/2}} \cos((1-\alpha)\lambda_n^{1/2}) \cos(q\alpha\lambda_n^{1/2}) \tag{18}$$

When combined with the expression for $g_{1,n}(\tau)$, eq 16, the time-dependent amount of oxygen in the sensor layer, $m_\alpha(\tau)$, is then given as

$$m_\alpha(\tau) = \sum_{n=0}^{\infty} \frac{2S \cos^2(q\alpha\lambda_n^{1/2}) \cos((1-\alpha)\lambda_n^{1/2})}{\lambda_n \left(\frac{\alpha}{S} \sin^2((1-\alpha)\lambda_n^{1/2}) + (1-\alpha)\cos^2(q\alpha\lambda_n^{1/2}) \right)} \exp(-\lambda_n \tau) \quad \alpha \neq 1 \tag{19}$$

In turn, using this dimensionless expression, the experimentally measured sorption profile is written as

$$\frac{M(t)}{M(\infty)} = 1 - \frac{m_\alpha(\tau)}{\alpha} \tag{20}$$

where $M(\infty)$ is the amount of oxygen sorbed at an infinite time when the film has reached equilibrium with the ambient atmosphere.

Therefore, if the solubilities of oxygen in the respective polymers are known, eq 20 can be used in an iterative scheme to model our experimental sorption data and thus determine the oxygen diffusion coefficient in the sample layer.

Numerical Solution. In principle, the analytical solution described above could be tested with the numerical scheme developed, for example, by Hedenqvist and Gedde,[18] which is rather inclusive and capable of handling nonlinearities. On the other hand, given the linearity of our present system and, thus, for the sake of simplicity, we opted to model the bilayer problem using the Galerkin Finite Element Method with piecewise linear functions in each element.[28] The Galerkin method was implemented using the original formulation of the bilayer model (eqs 1 and 2) and the boundary conditions given in eqs 3−7 to ensure exact continuity of the diffusion flux at the phase boundary. As with the analytical solution, the concentration profiles obtained numerically were integrated to obtain a measure of the oxygen content in the sensor layer which, in turn, makes it possible to model our experimental sorption data.

Comparison between the Analytical and Numerical Solutions. The solution to the finite element equations was implemented in MATLAB,[27] and the result was obtained as the concentration profile of oxygen in the respective films at a given time t after exposure of the bilayer to a given pressure p of oxygen. Upon comparison with the results obtained using the analytical solution, the respective concentration profiles match extremely well (Figure 2). For example, for the concentration profile at $t = 45$ s illustrated in Figure 2, the difference between the two solutions is no greater than 0.005% at any given point on the profile.

It is important to note in Figure 2 that, for the parameters used in this simulation, there is a sharp increase in the concentration of oxygen at the boundary between the two layers (i.e., at the boundary, the oxygen concentration in the inner layer is higher than that in the outer layer exposed to the ambient atmosphere). In considering this result, one must recall the boundary condition expressed in eq 4. Specifically, it was stipulated that the partial pressure of oxygen in the system, as represented by the oxygen concentration divided by the oxygen solubility, should not change across the interface between the polymer layers. The concentration itself, however, is not continuous. Thus, at any time t after exposure of the sample to an atmosphere of oxygen, the concentration of oxygen in a given layer will scale with the solubility of oxygen in that layer. Under the present conditions, where $S_1 > S_2$, one thus observes a distinct increase in concentration upon moving across the boundary from the sample into the sensor layer. It is also important to note that the concentration gradient in the respective layers becomes less pronounced as t increases (i.e., as one more closely approaches equilibrium with the ambient atmosphere).

As an aside, one advantage of our numerical approach to the diffusion problem is the ability to consider films that consist of more than two layers. Of course, this requires that one consider additional equations analogous to those in eqs 1−7. Nevertheless, the solution to the resultant set of coupled differential equations is readily accommodated simply upon the addition of extra terms to the diagonalized matrixes used. A numerically simulated concentration profile for oxygen in a film consisting of three layers is illustrated in Figure 3.

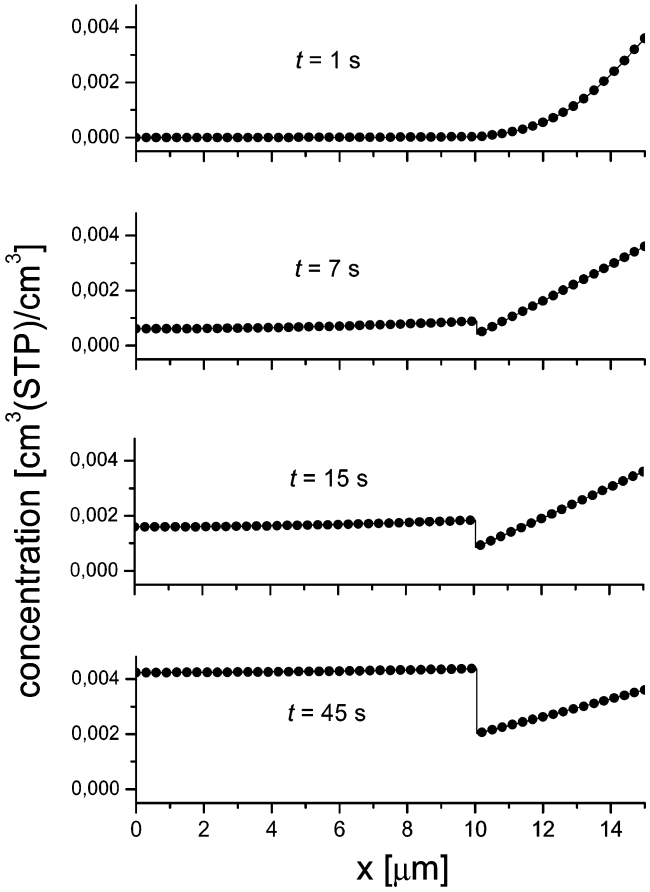

Figure 2. Simulated concentration profiles determined using the analytical (●) and numerical (–) solutions to the bilayer problem. For the latter, 100 elements were used. The concentration profiles were modeled using parameters similar to those encountered in our experimental study in which a film of poly(ethylene-*co*-norbornene) was cast onto a film of polystyrene. Layer 1: 10-μm thick; $D = 2.3 \times 10^{-7}$ cm^2 s^{-1}; $S = 0.2$ cm^3(STP) cm^{-3} atm^{-1}. Layer 2: 5-μm thick; $D = 2.2 \times 10^{-8}$ cm^2 s^{-1}; $S = 0.09$ cm^3(STP) cm^{-3} atm^{-1}. Concentration profiles have been calculated for four different elapsed times after exposure to an ambient atmosphere of 30 Torr oxygen.

In Figure 3, it is once again important to note that, for the parameters used in this simulation, the model indicates that the concentration of oxygen in the middle layer is higher than that in both the inner and outer layers. As explained previously with respect to the profiles modeled in Figure 2, this phenomenon reflects an oxygen solubility in the middle layer that is larger than that in the inner and outer layers, respectively.

2. Modeled Sorption Profiles. Before applying our general numerical solution for the bilayer problem to experimental sorption data, it is prudent to examine how it behaves under two limiting cases. Specifically, there are two circumstances in which the bilayer problem reduces to a simple one-layer problem that, in turn, can be modeled using independent solutions to Fick's second law for diffusion.

Limiting Case 1. In this circumstance, the thickness of the sample layer, $l_2 - l_1$, is assumed to be zero. Thus, the system is effectively reduced to a single layer film with a thickness l for which the time-dependent sorption profile is given by eq 21[8,22]

$$\frac{M(t)}{M(\infty)} = 1 - \sum_{n=0}^{\infty} \frac{8}{(2n+1)^2\pi^2} \exp\left(\frac{-D(2n+1)^2\pi^2 t}{4l^2}\right) \tag{21}$$

Equation 21 was used to model the time-dependent oxygen

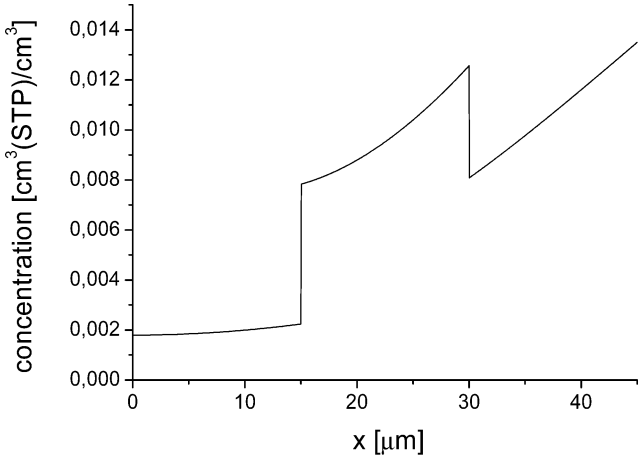

Figure 3. Simulated concentration profile, obtained using the finite element method, for oxygen sorption in a film that consists of three layers. The following parameters were used. Inner layer: 15 μm thick; $D = 4.3 \times 10^{-7}$ cm^2 s^{-1}; $S = 0.15$ cm^3 (STP) cm^{-3} atm^{-1}. Middle layer: 15 μm thick; $D = 2.0 \times 10^{-7}$ cm^2 s^{-1}; $S = 0.53$ cm^3 (STP) cm^{-3} atm^{-1}. Outer layer: 15 μm thick; $D = 3.0 \times 10^{-7}$ cm^2 s^{-1}; $S = 0.34$ cm^3 (STP) cm^{-3} atm^{-1}. This plot models the concentration profile 15 s after exposure of the trilayer film to 30 Torr of oxygen.

sorption profile into a 10-μm-thick film with $D = 1 \times 10^{-8}$ cm^2 s^{-1}. Independently, the general numerical solution to the bilayer problem was used to likewise model the time-dependent sorption profile under this particular limiting condition of $l_2 - l_1 = 0$ (as discussed above, the concentration profile obtained from the finite element method was simply integrated to obtain a measure of the overall oxygen content in the film). As shown in Figure 4a, the correlation between the simulated sorption profiles is excellent.

As an aside, with respect to the analytical solution to the bilayer problem, this limiting case of $l_2 - l_1 = 0$ corresponds to $\alpha = 1$ in which case the eigenvalues are given by $q\lambda_n^{1/2} = \pi(2n + 1)/2$. Although the expression in eq 19 is not defined for $\alpha = 1$, it can nevertheless be rewritten to show that the limiting form for $\alpha \rightarrow 1$ indeed, through eq 20, corresponds to the expression in eq 21.

Limiting Case 2. In this circumstance, we consider the opposite limit in which $\alpha \rightarrow 0$. In this situation, the sensor layer is so thin that it is essentially in equilibrium with the sample layer at the sensor−sample interface (i.e., the sensor layer is, in effect, not a receiving volume). In this limit, it can be shown from eq 14 that the eigenvalues are given by

$$\lambda_n^{1/2} = \pi(2n + 1)/2$$

and that

$$\lim_{\alpha \rightarrow 0} \frac{\cos((1 - \alpha)\lambda_n^{1/2})}{\alpha} = \frac{(-1)^n \pi(2n + 1)}{2S} \qquad (22)$$

In turn, the limiting form of the sorption expression becomes

$$\frac{M(t)}{M(\infty)} = 1 - \frac{4}{\pi} \sum_{n=0}^{\infty} \frac{(-1)^n}{(2n + 1)} \exp\left(\frac{-D_2(2n + 1)^2 \pi^2 t}{4l_2^2} \right) \qquad (23)$$

The expression in eq 23 is equivalent to that obtained by other investigators for the corresponding conditions.[16,22]

Equation 23 was used to model the time-dependent oxygen sorption profile through a 25-μm-thick sample film in which $D = 1 \times 10^{-8}$ cm^2 s^{-1}. Independently, the general numerical solution to the bilayer problem was used to likewise model the time-dependent sorption profile under this limiting condition of no flux across the sensor-sample interface. (In this latter case, the following parameters were used: layer 1 (sensor), 1 μm thick, $D = 1 \times 10^{-7}$ cm^2 s^{-1}; layer 2 (sample), 25 μm thick, $D = 1 \times 10^{-8}$ cm^2 s^{-1}. The ratio of oxygen solubilities, S_2/S_1, was 10.) As shown in Figure 4b, the correlation between the simulated sorption profiles is, once again, excellent.

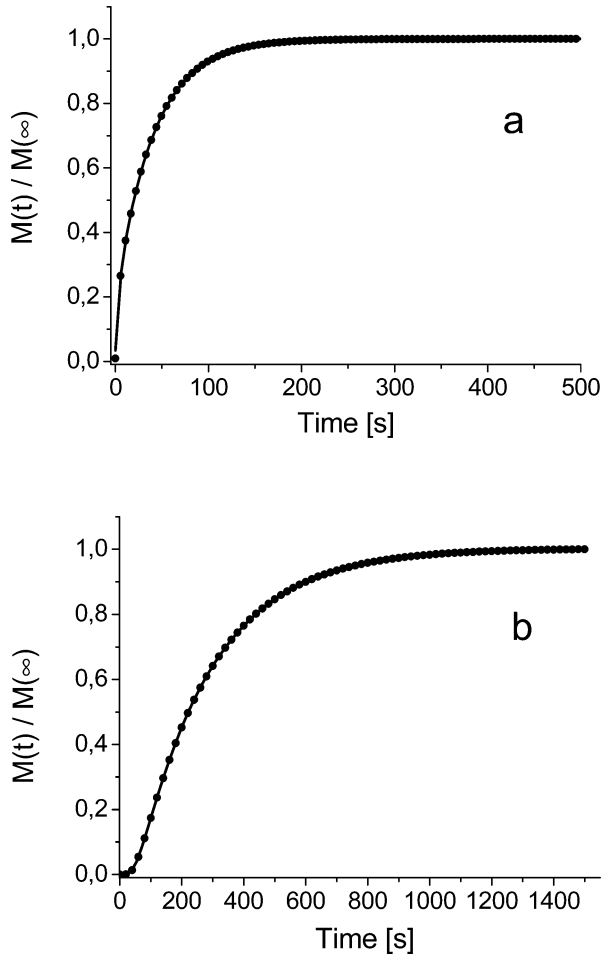

Figure 4. Computer-generated, time-dependent oxygen sorption profiles for the limiting cases in which (a) the thickness of the sample layer is reduced to 0 and (b) the flux across the sample−sensor interface is 0. Traces simulated using the general numerical solution to the bilayer problem (●) are seen to correlate extremely well with traces independently generated using equations applicable only to these limiting cases (—).

In conclusion, the general numerical solution for oxygen diffusion in bilayer films appears to accurately describe diffusion under two important limiting cases.

3. Experimental Sorption Profiles

Bilayer polymer films were prepared on a glass substrate. In this study, a film of poly(ethylene-*co*-norbornene) was cast on top of a film of polystyrene doped with *meso*-tetraphenylporphine (TPP). The solvents used to spin cast these respective films were chosen such that appreciable interdiffusion of the respective polymers at the polymer−polymer interface should not occur. In a given experiment, the rate of oxygen sorption into the inner, polystyrene sensor layer was monitored upon exposure of the outer, poly(ethylene-*co*-norbornene) sample layer to a specific partial pressure of oxygen (Figure 5).

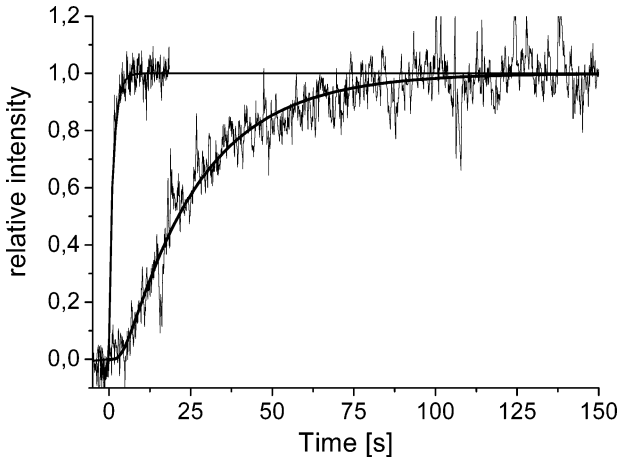

Figure 5. Intensity of singlet oxygen phosphorescence recorded from degassed polymer films exposed, at $t = 0$, to 30 Torr of oxygen. Data recorded from a 10-μm-thick film of TPP-doped polystyrene are shown in the fast-rising trace on the left. The slow-rising trace on the right shows data recorded from a bilayer system in which a 5-μm film of poly(ethylene-*co*-norbornene) was cast on top of a 10-μm polystyrene film. The solid lines superimposed on the experimental data were obtained using the numerical solution to the diffusion problem.

In independent sorption experiments performed on single films at 25 °C, we have ascertained that the oxygen diffusion coefficient in polystyrene, $D(\mathrm{PS}) = (2.3 \pm 0.2) \times 10^{-7}$ cm^2 s^{-1}, is approximately 1 order of magnitude larger than the oxygen diffusion coefficient in this particular copolymer of ethylene and norbornene, $D(\mathrm{EcN}) = (2.2 \pm 0.3) \times 10^{-8}$ cm^2 s^{-1}.[8,9,19] These results are consistent with the data shown in Figure 5. Specifically, upon exposure of a degassed 10-μm-thick polystyrene film to oxygen, the rate of oxygen sorption is comparatively rapid, and the film reaches equilibrium with the surrounding atmosphere within ~5 s. On the other hand, upon coating the polystyrene sensor layer with a 5-μm-thick film of poly(ethylene-*co*-norbornene), the rate of oxygen sorption into the sensor layer decreases substantially. In this latter case, it takes approximately 100 s to reach equilibrium with the surrounding atmosphere.

As discussed in section 1, to implement either the analytical or numerical solutions to the bilayer problem in which the diffusion coefficient in the sample layer is not known, it is necessary to have values for the solubility of oxygen in both polymer layers and a value for the oxygen diffusion coefficient in the sensor layer. Although oxygen solubility data are available in the literature for polystyrene, $S(\mathrm{PS}) = 0.18 \pm 0.02$ cm^3 (STP) cm^{-3} atm^{-1},[29,30] values for the solubility of oxygen in copolymers of ethylene and norbornene are not available. To this end, we performed independent experiments to quantify the solubility of oxygen in films of poly(ethylene-*co*-norbornene) using traditional permeability measurements.[19] On the basis of this work, we obtained an oxygen solubility in our copolymer of ethylene and norbornene, $S(\mathrm{EcN})$, of 0.09 ± 0.03 cm^3 (STP) cm^{-3} atm^{-1}. By use of our sorption method, values for the oxygen diffusion coefficient in polystyrene were likewise independently determined for each sensor film prior to depositing the poly(ethylene-*co*-norbornene) sample layer.

Upon incorporation of these parameters into the numerical solution to the diffusion problem, we were able to model the experimental data quite well (Figure 5). The best fits of the simulated sorption trace to data recorded from four separate bilayer films, each of a different thickness, were obtained using a value for the diffusion coefficient in poly(ethylene-*co*-norbornene), $D(\mathrm{EcN})$, of $(4.6 \pm 0.5) \times 10^{-8}$ cm^2 s^{-1} (Table 1).

TABLE 1: Oxygen Diffusion Coefficients, *D*(EcN), in Poly(ethylene-*co*-norbornene) Obtained from a Sorption Experiment in a Bilayer System

bilayer	thickness of sensor layer (μm)	thickness of bilayer (μm)	$D(\mathrm{EcN})^a$ (cm^2 s^{-1})
1	10.1 ± 0.1	15 ± 1	$(4.3 \pm 0.5) \times 10^{-8}$
2	10.2 ± 0.2	14.9 ± 0.1	$(4.9 \pm 0.5) \times 10^{-8}$
3	10.1 ± 0.1	15.4 ± 0.5	$(4.8 \pm 0.5) \times 10^{-8}$
4	10.2 ± 0.2	22 ± 3	$(4.2 \pm 0.8) \times 10^{-8}$

[a] For each value of D, the error cited derives solely from the error in the thickness of the respective layers. Specifically, these numbers do not reflect the error in the oxygen solubilities in the respective layers.

This value for $D(\mathrm{EcN})$ is to be compared with that independently obtained using our oxygen sorption technique on a single film of the copolymer, $D(\mathrm{EcN}) = (2.2 \pm 0.3) \times 10^{-8}$ cm^2 s^{-1}, and with that obtained from a traditional "time-lag" permeation measurement on a thicker, bulk sample of the copolymer, $D(\mathrm{EcN}) = (3.9 \pm 1.4) \times 10^{-8}$ cm^2 s^{-1}.[19]

In examining these values of $D(\mathrm{EcN})$, it is important to note several points. First, it is clearly indicated in Table 1 that, despite a comparatively poor signal/noise ratio in our sorption data (Figure 5), the experiments using different bilayer samples all yield the same result. Thus, in the least, our experiments and associated fitting routine are precise. Second, in reporting errors on the respective values of $D(\mathrm{EcN})$ obtained in the bilayer experiment, we opted to only consider the error that derives from the uncertainty in the thickness of the respective layers. Specifically, when using the numerical model to simulate the oxygen sorption profile, we have not incorporated any error associated with the solubilities of oxygen in both polystyrene and poly(ethylene-*co*-norbornene). Given that the numerical solution is quite sensitive to the values of S used and given that the solubility of oxygen in the films used in the bilayer experiment is likely to be somewhat different than that in the films used to independently quantify S (i.e., parameters such as D and S vary significantly on the history of the given sample),[19] we conclude that the value of $D(\mathrm{EcN})$ obtained in the bilayer experiment is accurate.

4. Deviations from Henry's Law

In the development of both the analytical and numerical solutions to the bilayer problem, we assumed that the concentration of oxygen in the polymer obeyed Henry's law. This was specifically embodied in the boundary condition stating that the oxygen concentration at the surface of the outer polymer layer, c_2, is always directly proportional to the external pressure of oxygen, p (eq 3). It is well known, however, that the pressure dependence for gas sorption in many glassy polymeric materials can be more complicated, particularly at low pressures.[11,31−33] Under these circumstances, a second pressure-dependent term is commonly added to the Henry's law term in attempts to quantify gas sorption. In this regard, the use of a Langmuir-type sorption isotherm has been quite successful in expressing the concentration, c, of sorbed gas (eq 24)

$$c = K_{\mathrm{H}}p + K_{\mathrm{L}}\frac{bp}{1 + bp} \tag{24}$$

This pressure-dependent phenomenon is usually described in the context of the so-called "dual-mode" sorption model.[31−33] Specifically, the Langmuir term is believed to describe gas sorption in microcavities or voids that are unique to glassy polymers (the parameter b in eq 24 is generally referred to as a void affinity constant). As the pressure p is increased, the

Langmuir domain of microcavities will eventually saturate, and Henry behavior will then be observed in that the amount of sorbed gas will depend linearly on the ambient pressure.

In independent experiments, we have established that oxygen sorption in a number of glassy polymers is indeed consistent with the dual-mode model.[9−11] Moreover, our spectroscopic probe of oxygen sorption is uniquely sensitive to the effects of dual-mode sorption simply because these experiments must generally be performed at ambient gas pressures less than ∼100 Torr.[8,11]

With respect to the current bilayer problem, the oxygen sorption data shown in Figure 5 were recorded upon exposure of the sample to 30 Torr of oxygen. Thus, it is indeed likely that the numerical solution used to model the data is inherently flawed based solely on the assumption that Henry's law is obeyed in this system. This flaw could possibly contribute, in part, to the slight difference between values of D(EcN) obtained in the bilayer experiment and those independently obtained in experiments on single films. Nevertheless, as we concluded in the previous section, the value of D(EcN) obtained from the bilayer experiment appears to be reasonably accurate. Thus, the limitation inherent to the numerical model associated with the neglect of nonlinear sorption terms will probably not become apparent until a better signal/noise ratio can be obtained in the experimental data.

It is perhaps also worthwhile to note that, in establishing our boundary conditions, we assumed that the partial pressure of oxygen does not change across the sensor−sample interface (eq 4). This implies that gas exchange is fast between the respective layers and that equilibrium is maintained at the interface. The data obtained in our study are indeed consistent with a model based on this presumed equilibrium. Thus, at present and for these particular phase-separated systems, it appears unnecessary to consider the more complicated case where transport across the phase boundary is slow and an equilibrium is not maintained.[34]

Conclusions

Experiments have been performed to quantify oxygen diffusion in bilayer polymer films. By use of the phosphorescence of singlet oxygen as a spectroscopic probe, the time evolution of oxygen transport through an outer sample layer and into an inner sensor layer was monitored. The data were modeled using both analytical and numerical solutions to Fick's second law of diffusion for the bilayer system. The results indicate that this spectroscopic technique can indeed be used to obtain an accurate oxygen diffusion coefficient for the outer sample layer in a bilayer film.

Acknowledgment. This work was supported by grants from the Materials Research Program of the Danish Research Council and from the Danish Polymer Centre. The authors thank Toivo Kodas and Arthur Baca for insight during the early stages of this project. The authors also thank Dieter Ruchatz of Hoechst Ticona (Germany) for the gift of TOPAS 8007.

References and Notes

(1) *Diffusion in Polymers*; Neogi, P., Ed.; Marcel Dekker: New York, 1996.
(2) Vieth, W. R. *Diffusion In and Through Polymers*; Oxford University Press: New York, 1991.
(3) *Polymeric Gas Separation Membranes*; Paul, D. R., Yampol'skii, Y. P., Eds.; CRC Press: Boca Raton, 1994.
(4) *Barrier Polymers and Structures*; Koros, W. J., Ed.; ACS Symposium Series; American Chemical Society: Washington, DC, 1990; Vol. 423.
(5) Sawyer, D. T. *Oxygen Chemistry*; Oxford University Press: New York, 1991.
(6) Schnabel, W. *Polymer Degradation*; Macmillan/Hanser: New York, 1981.
(7) Grassie, N.; Scott, G. *Polymer Degradation and Stabilisation*; Cambridge University Press: Cambridge, 1985.
(8) Gao, Y.; Ogilby, P. R. *Macromolecules* **1992**, *25*, 4962−4966.
(9) Gao, Y.; Baca, A. M.; Wang, B.; Ogilby, P. R. *Macromolecules* **1994**, *27*, 7041−7048.
(10) Wang, B.; Ogilby, P. R. *Can. J. Chem.* **1995**, *73*, 1831−1840.
(11) Poulsen, L.; Ogilby, P. R. *J. Phys. Chem. A* **2000**, *104*, 2573−2580.
(12) Ogilby, P. R.; Dillon, M. P.; Gao, Y.; Iu, K.-K.; Kristiansen, M.; Taylor, V. L.; Clough, R. L. *Adv. Chem. Ser.* **1993**, *236*, 573−598.
(13) Ogilby, P. R.; Kristiansen, M.; Clough, R. L. *Macromolecules* **1990**, *23*, 2698−2704.
(14) Scurlock, R. D.; Ogilby, P. R. *J. Phys. Chem.* **1989**, *93*, 5493−5500.
(15) Petrak, K. *J. Appl. Polym. Sci.* **1979**, *23*, 2365−2371.
(16) Rharbi, Y.; Yekta, A.; Winnik, M. A. *Anal. Chem.* **1999**, *71*, 5045−5053.
(17) Massey, L. K. *Permeability Properties of Plastics and Elastomers: A Guide to Packaging and Barrier Materials*, 2nd ed.; Plastics Design Library: Norwich, 2003.
(18) Hedenqvist, M. S.; Gedde, U. W. *Packag. Technol. Sci.* **1999**, *12*, 131−141.
(19) Poulsen, L.; Zebger, I.; Klinger, M.; Eldrup, M.; Sommer-Larsen, P.; Ogilby, P. R. *Macromolecules* **2003**, *36*, 7189−7198.
(20) Slayter, E. M.; Slayter, H. S. *Light and Electron Microscopy*; Cambridge University Press: Cambridge, 1992.
(21) Parkhutik, V.; Martinez, M. S.-J.; Senent, E. G. *J. Porous Mater.* **2000**, *7*, 239−242.
(22) Crank, J. *The Mathematics of Diffusion*, 2nd ed.; Oxford Press: Oxford, 1975.
(23) Carslaw, H. S.; Jaeger, J. C. *Conduction of Heat in Solids*, 2nd ed.; Oxford University Press: Oxford, 1946.
(24) Barrie, J. A.; Levine, J. D.; Michaels, A. S.; Wong, P. *Trans. Faraday Soc.* **1963**, *59*, 869−878.
(25) Wylie, C. R.; Barret, L. C. *Advanced Engineering Mathematics*; McGraw-Hill: New York, 1982.
(26) Conte, S. D.; deBoor, C. *Elementary Numerical Analysis*; McGraw-Hill: New York, 1965.
(27) MATLAB.; Mathworks, Inc.: Natick, MA.
(28) Ciarlet, P. G. *The Finite Element Method for Elliptic Problems*; North-Holland Publishing Company: Amsterdam, 1987.
(29) Yasuda, H.; Stannett, V. In *The Polymer Handbook*, 2nd ed.; Brandrup, J., Immergut, E. H., Eds.; Wiley: New York, 1975; pp III-229−III-240.
(30) Peterson, C. M. *J. Appl. Polym. Sci.* **1968**, *12*, 2649−2667.
(31) Koros, W. J. *J. Polym. Sci.: Polym. Phys. Ed.* **1980**, *18*, 981−992.
(32) Paul, D. R. *Ber. Bunsen-Ges. Phys. Chem.* **1979**, *83*, 294−302.
(33) Zhou, S.; Stern, S. A. *J. Polym. Sci. B: Polym. Phys.* **1989**, *27*, 205−222.
(34) Barzykin, A. V.; Tachiya, M. *J. Phys. Chem. B* **1998**, *102*, 3192−3197.